Calculation of intersubband absorption in n-doped $BaSnO_3$ quantum wells

Novak Stanojević, Jelena Radovanović, Nikola Vuković
IEEE Conference Publishing
University of Belgrade, School of Electrical Engineering,
Bulevar kralja Aleksandra 73, 11120 Belgrade, Serbia
nvukovic@etf.bg.ac.rs

Abstract- In this work we explore novel and promising $BaO/BaSnO_3$ perovskite-oxide quantum well material system which has recently attracted attention due to its many advantages and possible applications in electronic devices. We focus on calculation of intersubband absorption in La-doped $BaSnO_3$ quantum wells and investigate the tuning of absorption spectra with QW thickness and external electric field along the growth direction of the heterostructure.

I. INTRODUCTION

Recent studies performed on $BaO/BaSnO_3$ quantum wells (QWs) demonstrate the advantages of perovskite-oxide (PO) based QWs over traditional semiconductor QWs in terms of strong optical nonlinearities [1, 2]. Lightly La-doped $BaSnO_3$ (BSO) has very high room-temperature conductivity and wide band gap (4eV), which makes it attractive for novel transparent conductors and high-power electronic devices [3-6]. La-doped BSO also has a very small electron effective mass ($0.17m_0$) due to large curvature of the Sn $5s$-based conduction band (CB) bottom. A very large conduction band offset enables greater control of the QW properties. In addition, the giant nonlinear optical susceptibility that exists across a broad spectral range, makes BSO QWs applicable in a wide range of frequencies from THz to near-visible light.

[1]In this contribution we analyze double QW (DQW) and triple QW (TQW) where the well and barrier layers consist of BSO and BaO materials respectively. Both the DQW and the TQW are surrounded by thick BaO barrier layers (see insets of Figs. 1 and 2).

The electronic structure is obtained from 1D effective mass Schrödinger equation:

$$-\frac{\hbar^2}{2}\frac{d}{dz}\frac{1}{m(z)}\frac{d\Phi_i(z)}{dz}+U_{eff}(z)\Phi_i(z)=E_i\Phi_i(z) \quad (1)$$

where $m(z)$ is the effective mass along the growth direction, and $\Phi_i(z)$ is the envelope function (EF). The total effective potential $U_{eff}(z) = U(z)+\varphi(z)$ consists of $U(z)$, which is the conduction band offset between BSO and BaO (~1.74 eV), and the added electrostatic potential $\varphi(z)$ due to the La-doping, found by solving the Poisson equation:

$$\frac{d^2\varphi(z)}{dz^2}=\frac{e}{\varepsilon}\big(n(z)-N_d(z)\big) \quad (2)$$

where $N_d(z)$ is the La-doping density. The assumption has been made as in [1] that the ions of the dopants are evenly distributed across the entire heterostructure. In our simulations we use average doping densities of $N_d = 10^{19}cm^{-3}$ and $N_d = 5\times10^{18}cm^{-3}$ for the DQW and TQW respectively [3]. Electron density $n(z)$ is given by: $n(z) = \sum_i N_{s,i}|\Phi_i(z)|^2$ where $N_{s,i}$ is the sheet carrier density i.e. number of electrons per unit cross-section area in the i-th state. The corresponding coupled Schrödinger-Poisson (SP) system of equations is solved self-consistently [7].

The energies and wave functions of the bound states found from SP solver are used to calculate the linear optical absorption $A(\hbar\omega)$ for the intersubband transitions:

$$A_{if}(\hbar\omega)=\frac{e^2\omega\pi}{\varepsilon_0 n_r rc}\big(N_{s,i}-N_{s,f}\big)\big|d_{if}\big|^2L(\hbar\omega) \quad (3)$$

where n_r is the refractive index, d_{if} is dipole matrix element $d_{if}=\int_0^{L_z}\Phi_i^* z\Phi_f\,dz$, and L_z is the total length of the structure. The Lorentzian $L(\hbar\omega)$ is expressed as: $L(\hbar\omega) = \frac{1}{2\pi}\Gamma_{if}\Big/\Big[\big(E_f(0)-E_i(0)-\hbar\omega\big)^2+\big(\frac{\Gamma_{if}}{2}\big)^2\Big]$ with its width Γ_{if} estimated to be 10% of the energy difference between the final and initial states.

We further analyze the dependence of the fractional absorption $A(\hbar\omega)$ on the thickness of the well layers for the DQW and the TQW. Finally, we include an external electric field in order to see its effect on the optical absorption of the DQW.

II. RESULTS AND DISCUSSION

In this section we present the results of our numerical simulations. Since the largest absorption is achieved in symmetrical structures, in this contribution we limit our considerations to symmetrical structures only. We vary the layers' thickness in the multiples of the lattice parameter (unit cell) of BSO which is 4.10 Å.

The inset of Fig. 1. shows the results of the SP solver, namely effective potential $U_{eff}(z)$ and wave functions that correspond to the symmetric DQW with well thickness (cw)

[1] This work was supported by Ministry of Education, Science and Technological Development (Republic of Serbia).

of 5 unit cells and barrier thickness of 1 unit cell. Fig. 1 illustrates the largest absorption peak $\boldsymbol{A_{12}}$ (transition between the first and the second subband, denoted by the red and orange wave functions in the inset) for the three values of cw: 4 unit cells (blue spectrum, full line), 5 unit cells (red spectrum, dashed line), and 6 unit cells (orange spectrum, dash-dotted line). QWs are separated by a 1 unit cell thick barrier layer in all cases. The Fermi level (not shown) is just above the second subband denoted by the orange wave function in the inset. From Fig. 1 we can see that the increase in the QW width results in the decrease of energy at which absorption transition A_{12} occurs.

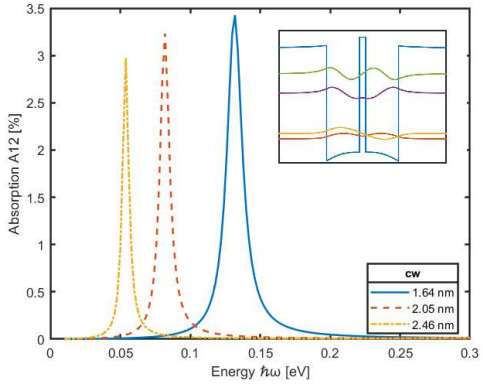

FIG. 1. Absorption spectra for symmetric DQW, where only the largest peak A_{12} is shown, for well thickness (cw) being 4, 5 and 6 unit-cells (1.64, 2.05 and 2.46 nm), while the barrier thickness is 1-unit cell (0.41 nm).

The inset of Fig. 2. shows the effective potential $U_{eff}(z)$ and wave functions that correspond to the symmetric TQW with all 3 wells' thickness cw equal to 4 unit cells and barriers' thickness of 1 unit cell.

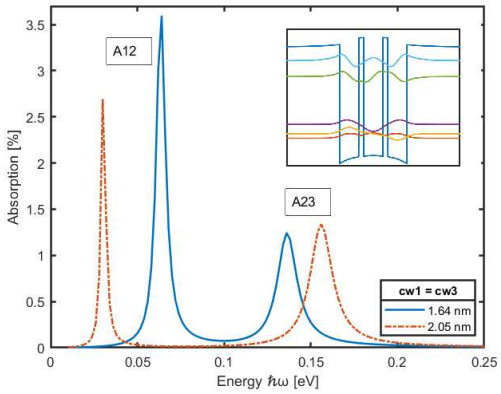

FIG. 2. Absorption spectrum for TQW, with the dominant A_{12} and A_{23} peaks shown (the Fermi level is just above the second subband) for both the first and third well layers being four- and five- unit-cell thick (1.64, 2.05 nm), while the second well layer was four-unit cell thick (1,64 nm) and both of the barrier layers were one-unit cell thick(0.41 nm).

Fig. 2 illustrates the two dominant absorption peaks $\boldsymbol{A_{12}}$ (transition between the first and second subband denoted by the red and orange wave functions in the inset) and $\boldsymbol{A_{23}}$ (transition between the second and third subband denoted by the orange and purple wave functions in the inset) for the two values of left/right QW widths: 4 unit cells (blue spectra, full line), and 5 unit cells (red spectra, dash-dotted line), while the middle QW is 4 unit cells thick. QWs are separated by 1 unit cell thick barriers. The Fermi level (not shown) is just above the second subband denoted by the orange wave function in the inset. From Fig. 2 we see the resulting shift in energies at which absorption transitions A_{12} and A_{23} occur, with the increase in the QW width.

The effect of an external electric field on absorption in DQW with well layers four-unit-cells thick, and the barrier layer one-unit thick can be seen in Fig. 3. The energy of the absorption transition increases with the electric field applied in the QWs' growth direction.

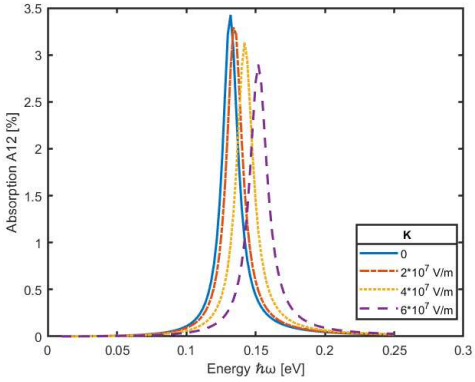

FIG.3. Absorption spectrum for DQW (the well layers were four-unit-cell thick, and the barrier layer one-unit thick), where only the largest peak A_{12} is shown (the Fermi level is just above the second subband) for different values of external electric fields.

III. CONCLUSION

In this work we have focused on the intersubband absorption calculation in QWs realized in n-doped BSO, a promising transparent conductive oxide with superior electron conductivity and wide optical band gap, in order to determine its potential for realization of devices based on intersubband transitions. Our initial study presented partially in this contribution suggests that high level of manipulation with absorption spectra is possible by changing layer thickness and turning of external electrical field. In future work we will consider barriers of materials other than BaO, and also include exchange-correlation effect when self-consistently solving SP system.

REFERENCES

[1] W. Li, A. K. Hamze, and A.A. Demkov, "Tunable giant nonlinear optical susceptibility in BaSnO3 quantum wells," *Phys. Rev. B* 104, 235419 (2021).
[2] W. Guo, "Transition Metal Oxide Thin Films Integration on $SrTiO_3$," Dissertation 2021.
[3] H. J. Kim et al., "Physical properties of transparent perovskite oxide (Ba,La)SnO3 with high electrical mobility at room temperature," *Phys. Rev. B* 86, 165205 (2012).
[4] H. J. Kim et al., "High Mobility in a Stable Transparent Perovskite Oxide," *Appl. Phys. Express* 5, 061102 (2012).
[5] H. R. Liu, J. H. Yang, H. J. Xiang, X. G. Gong and S. H. Wei, "High Mobility in a Stable Transparent Perovskite Oxide," *Appl. Phys. Lett.* 102, 112109 (2013).
[6] S. Raghavan et al., "High-mobility $BaSnO_3$ grown by oxide molecular beam epitaxy,", *APL Materials* **4**, 016106 (2016).
[7] Laurent Nevou (2022). Q_SchrodingerPoisson1D_CB (https://github.com/LaurentNevou/Q_SchrodingerPoisson1D_CB), GitHub. Retrieved March 18, 2022.